Using Kohn−Sham Orbitals in Symmetry-Adapted Perturbation Theory to Investigate Intermolecular Interactions

Hayes L. Williams and Cary F. Chabalowski*

Army Research Laboratory, AMSRL-WM-BD, Aberdeen Proving Ground, Maryland 21005-5006

Received: October 20, 2000

This is the first reported use of a hybrid method involving density functional theory (DFT) and symmetry-adapted perturbation theory (SAPT) to calculate intermolecular interactions. This work was stimulated by the reported failures of supermolecular DFT calculations to adequately predict intermolecular (and interatomic) interactions, particularly of the van der Waals type. The goals are to develop a hybrid scheme that will calculate intermolecular interaction energies accurately and in a computationally efficient fashion, while including the benefits of the energy decomposition provided by SAPT. The computational savings result from replacing the costly perturbation theory treatment with DFT, which should include the intramolecular correlation effects on the intermolecular interaction energies. The accuracy of this new hybrid approach (labeled SAPT(DFT)) is evaluated by comparisons with higher level calculations. The test cases include He_2, Ar_2, $Ar-H_2$, $(H_2O)_2$, $(HF)_2$, CO_2-CH_3CN, and CO_2-dimethylnitramine. The new approach shows mixed results concerning the accuracy of interaction energies. SAPT(DFT) correctly predicts all the qualitative trends in binding energies for all test cases. This is particularly encouraging in dimer systems dominated by dispersive interactions where supermolecular DFT fails to predict binding. In addition, the method achieves a drastic reduction (a factor of at least 100) in computational time over the higher level calculations often used to predict these forces. With respect to quantitative accuracy, this initial hybrid scheme, using the very popular exchange-correlation functional B3LYP, overestimates the second-order energy components (e.g., induction and dispersion terms) for all of the test cases, and subsequently overestimates the total interaction energy for all dimer systems except those heavily dominated by the electrotstatic interactions. The SAPT energy decomposition points to the use of DFT virtual orbital eigenvalues in the second-order perturbation terms as the likely cause for this error. These results are consistent with earlier work suggesting that DFT canonical virtual orbital energies obtained from commonly used functionals are less than optimal for use in such a perturbative scheme. The first-order interaction energy terms from the SAPT(DFT) are found to be generally more accurate than the second-order terms, and agree well with the benchmark values for dimers containing molecules with a permanent electric dipole moment. These first-order terms depend only upon the occupied MO eigenvectors, and hence are not affected by the inaccuracies in the Kohn−Sham DFT virtual orbital eigenvalues. These observations encourage future studies utilizing newly reported functionals, some of which have been developed to directly address problems with DFT virtual orbital energies and the asymptotic region of the electron density.

I. Introduction

This work attempts to fulfill a need in theoretical chemistry, i.e., the development of a new quantum chemistry approach for studying weak chemical interactions between large molecular systems, with the additional expectation that we can predict intermolecular interaction energies with the level of accuracy that is typically expected from correlated ab initio quantum chemical techniques. A reasonable starting point for such a development would be the Kohn−Sham[1,2] implementation of density functional theory (DFT).[1−5] While DFT has demonstrated impressive successes in predicting properties of isolated molecules, it has had less success in predicting intermolecular interaction energies.[6−9] "Exact" density functional theory applied to a collection of interacting molecules would include ALL correlation effects, including the dispersion forces. Unfortunately, the exact energy functionals of the density for molecules are unknown. Hence, all implementations of DFT to molecules depend on approximations to the exact energy functionals of the density. Studies have shown that for the commonly used exchange-correlation functionals, the London[10] dispersion forces are essentially neglected,[6] and some papers warn that even the results predicted for H-bonding interactions by DFT "... should be taken with care".[11] Recent work in the development of new exchange-correlation functionals has produced functionals fitted to many properties, including hydrogen bonded dimers.[12] Hence, these functionals would be expected to give improved H-bonding energies, at least for a category of H-bonded systems similar to the fitting set. To our knowledge, no such analogous work has been done to fit functionals to van der Waals complexes to produce functionals which better describe dispersive interactions. Whether this approach would be suitable for including dispersion interactions into DFT remains to be seen.

The inability to correctly account for dispersive interactions is a serious defect in DFT, and will drastically reduce its usefulness in important application areas such as biological research. In a review article on quantum mechanical techniques

* Corresponding author. E-mail: cary@arl.army.mil.

10.1021/jp003883p CCC: $20.00
Published on Web 12/29/2000

applied to the H-bonding and stacking of DNA base pairs, Sponer et al.[11] state "The stability of stacked pairs originates in the electron correlation (dispersion energy) ...". They also state that: "In view of the exponentially growing number of attempts to use DFT for biomolecules we have emphasize that the method completely fails for van der Waals complexes including stacked base pairs, and must be used with care, especially for biological molecules." If we wish to study biological systems (and any systems dominated by "van der Waals" interactions) with the expected accuracy of ab initio quantum chemical techniques, it seems imperative that a computationally tractable method such as DFT be available, and that some methodological improvements be made to correct for its inaccuracies in predicting dispersive and electrostatic interactions.

Kristyan and Pulay[6] recognized these shortcomings in the existing DFT methods, and have stated: 'Therefore, present DFT theories are probably not useful for the investigation of weakly interacting systems. In view of the good performance of modern density functional methods for the bulk of correlation effects, it is of considerable interest to develop hybrid methods which include the dispersion energy in DFT calculations." This current study addresses directly this need for a "hybrid" method, and takes the first step in developing and testing a new hybrid method.

It would be highly desirable for such a hybrid method to include the following attributes: (1) retain much of the computational expediency of the DFT method; (2) include the intermolecular correlations in a nonparametric (ab initio) fashion; (3) avoid the "double counting" of electron correlation effects, both for electrons interacting within a monomer and between monomers. (4) calculate the fundamental contributions to the intermolecular interactions, i.e., electrostatic, exchange, inductive and dispersive interaction energies, with equal accuracy; (5) ascertain the relative magnitudes for each of these components of the interaction energy.

The benefits of attributes (1−4) should be self-evident, and attribute (5) would provide a more basic physical understanding for the nature of such interactions. In addition, these components of the interaction energy could then be used in developing more accurate (and meaningful?) classical potential energy functions ("molecular force fields") for subsequent use in classical molecular dynamics and Monte Carlo simulations of large molecular systems including biosystems.

Toward these ends, we have combined DFT with the well documented, ab initio symmetry-adapted perturbation theory (SAPT)[13−15] approach to calculating intermolecular interaction energies. Quite simply, the Kohn−Sham (KS) implementation of DFT has been used to produce KS molecular orbitals (MOs) and their corresponding MO eigenvalues for use as expansion functions and energy differences (respectively) in a many-body perturbation theory (MBPT) implementation of SAPT. The DFT method will be used to account for the electron correlations within each monomer (intramolecular correlation) involved in the intermolecular interactions. This will eliminate the most computationally intensive part of the calculations in a standard MBPT implementation of SAPT, hence retaining most of the computational expediency of DFT. It will be shown in a later section that this approach can reduce the computational time for a dimer system the size of CH_3CN-CO_2 by a factor of 100 or more! Such an enormous computational savings is the main driving force behind this study. These computational savings are obtained while predicting intermolecular interactions (including intermolecular electron correlation corrections) in a rigorously ab initio fashion (without the "double-counting" problem) by application of the MBPT implementation of the SAPT approach. This DFT−SAPT hybrid approach should exhibit the aforementioned five attributes. The issue then becomes the accuracy one can expect from a SAPT description of the interaction energy by using the monomer electron densities, and MO eigenvectors and eigenvalues derived from DFT with a given exchange-correlation functional.

The main goals of this study will be to first ascertain if this new hybrid method shows at least the correct qualitative behavior for the interaction energies, and second to evaluate its absolute accuracy with respect to predicting total interaction energies. The interaction energy decomposition that results from the SAPT method will be helpful in analyzing the sources for any error in the total interaction energies. In addition, the ability (or rather inability) of supermolecular DFT to adequately account for dispersive interactions between atomic and molecular systems will be further documented for a selection of commonly used exchange-correlation functionals. To gauge the performance of this new hybrid DFT−SAPT method, we will compare interaction energies calculated using this method with energies resulting from high-level calculations using the standard implementation of SAPT. This will be done for various atomic and molecular dimer systems, including He_2, Ar_2, $Ar-H_2$, $(H_2O)_2$, $(HF)_2$, and $(CO_2)-X$, where $X = CH_3CN$ and dimethylnitramine (DMNA). These systems cover a range of interaction energy types (in particular, dispersive versus electrostatic) and magnitudes. Finally, MOs and eigenvalues derived from a selection of popular exchange-correlation functionals will be tested to determine which, if any, provide suitable canonical orbitals and energies for this hybrid method.

II. DFT: Previous Attempts to Calculate van der Waals Forces

As proposed by Hohenberg and Kohn[1] and Kohn and Sham,[1,2] DFT[3−5] includes a description of the intrasystem electron correlation in an approximate way through the so-called exchange-correlation functional. The choice of this functional determines the accuracy limits of this method. As previously mentioned, DFT sometimes fails completely for van der Waals interactions.[6−9] As Lacks and Gordon[31] point out, this is not totally surprising because the currently popular exchange-correlation functionals have been tested mainly for strongly bound molecular systems and solids.

Gordon and Kim[32] (GK) developed what was probably the first method for investigating intermolecular interactions using DFT as a starting point. They made two basic assumptions of interest here. First, there are two distinguishable atomic densities that undergo no rearrangement or distortion when they are brought together. Second, the total system density simply equals the addition of the Hartree−Fock density of systems A and B. They proceeded to investigate a number of closed-shell atom−atom interactions. This theory does not result in a full inclusion of dispersion and induction effects as fluctuations in the uniform electron gas model are not included. These fluctuations are essential to describing these particular physical effects. Even so, as illustrated by the authors, this method produced reasonable results for atomic interactions; the only notable exception is the He_2 interaction for which this method does poorly. This basic method can be extended or modified in a variety of ways and more detail on extensions can found in Spackman[33] and Parr and Yang.[3]

One modification of the GK approach made by Radzio-Andzelm and Kolos[34−36] incorporated the exchange energy expression used in Jeziorski et al.[37] The total system density

now included, in addition to the sum of the unperturbed system A and B densities (the basic GK assumption), three terms which accounted for electron exchange between the two systems. This modification significantly improved the results, especially for He_2. Unfortunately, the dispersion component of the interaction energy was still not a natural result of the theory and had to be added separately in order to directly compare with experiment.

Another DFT approach to calculating the intermolecular dispersion forces has been developed in refs 38−41. All of these studies use essentially the same starting assumption as SAPT theory, namely that there are two *distinguishable* electron distributions for systems A and B. However, in these approaches the density−density response functions (susceptibilities) of the electron distributions are calculated with the further restriction (not present in SAPT) of nonoverlapping charge densities. These authors are then able to derive expressions for the van der Waals C_6 coefficient using DFT and the Casimir and Polder formulas.[42] Analogies between ref 42 and the SAPT dispersion component are further discussed in refs 13 and 15.

One of the most recent developments in DFT theory for inclusion of dispersion forces is the work of Kohn et al.,[43] who propose and test a method that divides the Coulombic interactions into two parts, i.e., a long-range and a short-range part. The long-range part includes the van der Waals interactions, and its contribution to the interaction energy is represented by the "adiabatic connection formula".[43] This equation is then transformed into a time dependent expression to avoid solving for the density−density response function via iterative procedures. Utilizing an "exact" KS exchange-correlation potential, V_{XC}, their results on the He−He integrated frequency-dependent susceptibility are in close agreement with the value determined from the "completeness sum rule", and their static susceptibility is also in very close agreement with the best theoretical value. Their predicted values of the van der Waals' constant C_6 for both H−He and He−He are in extremely close agreement with the best theoretical values (differing by less that 1%). When the exact V_{XC} was replace by an LDA V_{XC}, the value for the He−He C_6 coefficient was off from the best value by 28%. While this new approach is quite promising, its application to larger systems employing approximate V_{XC} must yet be explored.

There are at least three other methods for investigating weak intermolecular interactions using DFT that should be noted. Two are based on specific partitions of the electron density. Stefanovich and Truong[44] describe a method of embedded density functional theory designed to model adsorption on crystalline surfaces. In this method, the electron density is divided into a part for the cluster and a part for the adsorbate. The second method by Wesolowski and Weber[45] calculates weak interaction energies by first partitioning the electron density into two parts (in the case of a dimer interaction), density "d1" and density "d2", with each density being that of the isolated molecule. The KS operator is then divided into two parts, F_0 and F_1, where F_0 operates exclusively on the "nonfrozen" density d1, and F_1 describes the interaction of the two molecules by operating on both d1 and the "frozen" density d2 on the neighboring molecule. Through this procedure, F_1(d1,d2) provides a mechanism for relaxing d1 due to the presence of the neighboring molecule and its density d2. This was then followed by exchanging the assignments of d1 and d2 to the other molecule in the dimer pair, and again relaxing the density d1 in the presence of a frozen (but now improved) d2. This iterative scheme is then repeated until a predetermined convergence in energy is achieved. This approach gave interaction energies in close agreement with supermolecule DFT results for H_2 + NCH. They also examined the results of performing only a single iteration wherein the density on either H_2 or NCH was relaxed, but not both. They briefly described the qualitative differences in results between this presumably less accurate, noniterative approach and the fully iterative scheme. They were also able to show that the kinetic energy calculated through their definition of the kinetic energy coupling term was in good agreement with the supermolecular DFT kinetic energy, lending credence to their choice for the form of the nonadditive kinetic energy functional term.

In a third approach, Cioslowski and Lopez-Boada[46] report what could be a very important step in the general development of exchange-correlation functionals. The authors derived an apparently new, approximate electron−electron repulsion energy functional of the one-electron reduced density matrix that is reported to contain an explicit functional form for the dispersion energy. This dispersion energy term is not an add-on, but rather comes naturally out of the derivation of the functional, which uses the hypervirial theorem for a certain class of two-electron operators. While no applications of this new functional are reported, the authors state[46] that coding is underway to allow for its application to atoms and molecules.

III. Methods

A. Symmetry-Adapted Perturbation Theory: Background. The traditional theoretical method for calculating the intermolecular interaction energy E_{int} between two systems is the so-called supermolecular approach. In this method, the energies of the monomers E_A and E_B are subtracted from the energy of the dimer, E_{AB}, to give the total interaction energy E_{int} as

$$E_{int} = E_{AB} - (E_A + E_B) \tag{1}$$

Unfortunately, E_{int} is typically many orders of magnitude smaller than the system energies, and errors introduced by the applied approximations may be as large as the quantity sought. Even if the various theory and basis set truncation errors are smaller than the desired accuracy, the supermolecular method yields only one number, i.e., the total interaction energy, with no additional information about the physical nature of the interaction (e.g., electrostatic versus dispersive).

Symmetry-adapted perturbation theory (SAPT) was developed as an ab initio approach to *directly* investigate these weak interactions and has been successfully applied to systems such as Ar−H_2,[14,20] He−HF,[14] He−CO,[14] Ar−HF,[14] He−C_2H_2,[14] H_2−CO,[21] and $(H_2O)_2$ [22] (further examples can be found in refs 13, 14, and 30). Besides its potential for high accuracy, this theory provides a very physical picture of the intermolecular interaction potential energy surface since E_{int} is naturally partitioned into components resulting from the electrostatic, exchange, inductive, and dispersive interactions of the two systems. With a judicious choice of atomic orbital (AO) basis set,[23] SAPT components can also be computed faster than an equivalent level of ab initio theory using the supermolecular method. Unfortunately, even with this advantage, SAPT (and ab initio electron correlation methods in general) exacts a high computational cost, much of which is associated with calculating the intramolecular correlation corrections. This might be reduced significantly by incorporation of DFT to account for the intramolecular correlation corrections.

B. Symmetry-Adapted Perturbation Theory: Outline of the Theory. A detailed derivation and description of SAPT has

already been presented[13−15,24,30] and will not be repeated here. However, the current, abbreviated outline of the theory will be necessary in interpreting the results, and understanding the role played by DFT in determining E_{int}. The basic Hamiltonian used for SAPT is divided into two parts. The first, $H_0 = H_A + H_B$, represents the Hamiltonians for two *isolated* systems A and B. The second part is the intermolecular interaction operator V between the two systems. Adding the two gives the full system Hamiltonian $H = H_0 + V$. The SAPT zeroth-order wave function is the product of the two isolated monomer wave functions $\Psi = \Psi_A\Psi_B$. The interaction energy E_{int} can then be expanded in terms of this total Hamiltonian and wave function as

$$E_{int} = E^{(1)}_{elst} + E^{(1)}_{exch} + E^{(2)}_{pol} + E^{(2)}_{exch} \quad (2)$$

where the superscript indicates the perturbation order with respect to V. Each term in eq 2 has a physically motivated interpretation. The leading terms $E^{(1)}_{elst}$ and $E^{(1)}_{exch}$ can be interpreted as the classical electrostatic interaction energy and the energy effect of the resonance tunneling (quantum mechanical exchange) of electrons between the two interacting systems, respectively. The $E^{(1)}_{elst}$ is the first-order component of the general set of terms $E^{(i)}_{pol}$. Both the second-order polarization and exchange energies separate naturally into dispersion and induction components as

$$E^{(2)}_{pol} = E^{(2)}_{ind} + E^{(2)}_{disp} \quad \text{and} \quad E^{(2)}_{exch} = E^{(2)}_{exch-ind} + E^{(2)}_{exch-disp} \quad (3)$$

Equation 2 implicitly assumes full intramonomer electron correlation for each component. Because this is generally not possible for many-electron systems (with some exceptions being noted[25,26]), each interacting molecule must be expanded in orders of the intramonomer electron correlation operator W, which is the sum of Moeller−Plesset type fluctuation potentials, $W = W_A + W_B$, for systems A and B, respectively. The many-electron SAPT Hamiltonian H can then be expressed as a sum of operators $H = F + W + V$ where $F = F_A + F_B$ is the sum of the Fock operators for systems *A* and *B*. Standard Rayleigh−Schroedinger perturbation theory using this Hamiltonian results in the so-called "polarization" expansion. The corresponding exchange counterparts result from symmetry forcing[27] designed to impose the correct permutational behavior on the electrons between systems. An expansion of each *n*th-order (in V) polarization and exchange energy in powers of W can then be written as

$$E^{(n)}_{pol} = \sum_{l=0}^{\infty} E^{(nl)}_{pol} \quad \text{and} \quad E^{(n)}_{exch} = \sum_{l=0}^{\infty} E^{(nl)}_{exch} \quad (4)$$

where l indicates the order in W. It is worth emphasizing that eq 4 represents a computationally intensive, double perturbation expansion. As will be shown in Section III.D, the inclusion of DFT will eliminate the need for the expansion in W, providing a sharp reduction in computational effort.

In practice, these infinite series expansions must be truncated at some computationally tractable values of l and n. To indicate this point, we begin by dividing the infinite order series in eq 4 into two parts, such that the first term does not include any intramonomer electron correlation and the second term is truncated at the *k*th-order in W.

$$E^{(1)}_{exch}(k) = E^{(10)}_{exch} + \sum_{l=1}^{k} E^{(1l)}_{exch} \quad (5)$$

If the sum over l in the second term contains but a single perturbation order, this energy contribution will be represented as an arabic character with the value of l given as the second number in the superscript. Otherwise, if the sum contains more than one value of l, the energy sum will be represented more compactly by the greek letter epsilon, with the highest value of l appended parenthetically. For example, ${}^tE^{(22)}_{ind}$ contains only the $l = 2$ term, while $\epsilon^{(1)}_{exch}(2)$ is the sum of $E^{(11)}_{exch}$ and $E^{(12)}_{exch}$, that is

$$\epsilon^{(1)}_{exch}(k) = \sum_{l=1}^{k} E^{(1l)}_{exch} \quad (6)$$

Finally, as seen in eq 5, the sum of all calculated perturbation levels to a given energy term is represented by an arabic letter with the highest perturbation order appended parenthetically, i.e., $E^{(1)}_{exch}(2)$. Such partitions hold for each of the components: $E^{(1)}_{elst}$, $E^{(1)}_{exch}$, $E^{(2)}_{disp}$, $E^{(2)}_{ind}$, $E^{(2)}_{exch-disp}$, $E^{(2)}_{exch-ind}$.

The supermolecular Hartree−Fock (HF) interaction energy E^{HF}_{int} can be shown to be asymptotically equal to the sum of selected SAPT components[28] as

$$E^{HF}_{int} = E^{(10)}_{elst} + E^{(10)}_{exch} + E^{(20)}_{ind,resp} + E^{(20)}_{exch-ind,resp} + \delta E^{HF}_{int} \quad (7)$$

$$= E^{HF}_{SAPT,resp} + \delta E^{HF}_{int} \quad (8)$$

where the subscript resp indicates that these terms have been calculated with the inclusion of the coupled Hartree−Fock response of a perturbed system.[30] The remaining term δE^{HF}_{int} indicates all other higher-order induction and exchange-induction terms not currently part of the SAPT suite of codes, but are part of the supermolecular Hartree−Fock energy. We will always calculate δE^{HF}_{int} using the Boys−Bernardi counterpoise scheme.[29]

The correlated portion of the interaction energy is approximated in SAPT by

$$E^{CORR}_{int} = \epsilon^{(1)}_{elst,resp}(3) + \epsilon^{(1)}_{exch}(2) + {}^tE^{(22)}_{ind} + E^{(20)}_{disp} + \epsilon^{(2)}_{disp}(2) + E^{(20)}_{exch-disp} + E^{t(22)}_{exch-ind} \quad (9)$$

where the term ${}^tE^{(22)}_{ind}$ collects all of the *true* correlation effects from $E^{(22)}_{ind,resp}$.[30] This is the first correlated induction contribution and hence not included in E^{HF}_{int}. The ${}^tE^{(22)}_{exch-ind}$ component should quench the corresponding induction component, but is currently not coded. By scaling $E^{(20)}_{exch-ind,resp}$ by ${}^tE^{(22)}_{ind}/E^{(20)}_{ind,resp}$ our estimate of this term is

$${}^tE^{(22)}_{exch-ind} \approx E^{(20)}_{exch-ind,resp} \frac{{}^tE^{(22)}_{ind}}{E^{(20)}_{ind,resp}} \quad (10)$$

The $\epsilon^{(2)}_{exch-disp}(2)$ could be approximated in a similar fashion, but because $E^{(20)}_{exch-disp}$ quenches a relatively small part of $E^{(20)}_{disp}$,[30] effects of $E^{(2i)}_{exch-disp}$, with $i \geq 1$, are probably very small.

The total SAPT interaction energy, from its standard implementation, at the highest level of theory currently available will then be approximated by

$$E_{\text{int}} = E_{\text{int}}^{\text{HF}} + E_{\text{int}}^{\text{CORR}} \tag{11}$$

Interaction energies, both the total and its components, calculated from eq 11 will be referred to as the "benchmark SAPT" results. To explore the role played by intramolecular electron correlation (or rather, the lack thereof) on the intermolecular interaction energy, we define the SAPT interaction energy between two interacting Hartree−Fock atoms or molecules to be

$$E_{\text{int}}[0] = E_{\text{elst}}^{(10)} + E_{\text{exch}}^{(10)} + E_{\text{disp}}^{(20)} + E_{\text{ind}}^{(20)} + E_{\text{exch-disp}}^{(20)} + E_{\text{exch-ind}}^{(20)} \tag{12}$$

with a superscript SAPT added if the possibility of confusion with the supermolecular HF interaction energy exists. This level of SAPT implementation contains intermolecular correlation but *no* intramolecular correlation, and will be referred to as "SAPT-(HF)".

C. Density Functional Theory. The DFT energy of a system can be written as[1−3]

$$E = T_0 + \int \rho V_{\text{ext}} \mathrm{d}r + \frac{1}{2}\int\int \frac{\rho(r_1)\rho(r_2)}{r_{12}} \mathrm{d}r_1 \mathrm{d}r_2 + E_{\text{XC}}[\rho] \tag{13}$$

where T_0 is the kinetic energy of non-interacting, independent particles, V_{ext} represents the electrostatic field of the nuclei, and the third term represents the classical coulombic interaction of the electrons. The last term is called the exchange-correlation functional and incorporates the remaining "unknown" pieces of the exact DFT functional. In principle, the exact nonrelativistic solution to the problem (including the London dispersion forces) could be obtained if this term were known precisely. The last three terms on the right hand side of eq 13 can be grouped into an effective potential

$$V_{\text{eff}} = V_{\text{ext}} + V_{\text{coul}} + V_{\text{XC}} \tag{14}$$

where

$$V_{\text{coul}}(1) = \int \frac{\rho(r_2)}{r_{12}} \mathrm{d}r_2 \quad \text{and} \quad V_{\text{XC}} = \frac{\delta E_{\text{XC}}}{\delta \rho} \tag{15}$$

Equation 13 can then be compactly written as

$$E = T_0 + \int \rho V_{\text{eff}} \mathrm{d}r \tag{16}$$

Using this effective potential, an independent particle system of equations can be written as

$$-\frac{1}{2}\nabla^2 \varphi_i + V_{\text{eff}} \varphi_i = \epsilon_i \varphi_i \tag{17}$$

which will be solved self-consistently to find the minimum energy of eq 13 given the condition that

$$\rho(\vec{r}) = \sum_{i=1}^{N} |\varphi_i(\vec{r})|^2 \tag{18}$$

where N is the total number of *occupied* orbitals in the system.

D. Combining Density Functional Theory with SAPT. It is important to state at the outset that absolutely no modifications were made to the DFT energy expression as programmed in the Gaussian[50] codes to facilitate the use of DFT with SAPT in this study. The basic steps used to "connect" DFT with SAPT are formally identical to the steps used to "connect" HF theory with SAPT as detailed in earlier papers describing SAPT.[13,14,30] In both approaches, the same 1-electron and 2-electron integrals over atomic orbitals are used to form a Hamiltonian matrix. These include the 1-electron kinetic energy and electron−nucleus attraction integrals, and the 2-electron coulomb repulsion integrals. In HF theory, the exchange energy is introduced during the formation of the Fock matrix through the HF operator and the spin properties associated with each spin−orbital. Likewise, in DFT, the exchange-correlation energy is incorporated into the KS equations during the formation of the KS matrix through the use of the KS operator, which includes an exchange-correlation operator operating on the spin−orbitals. Therefore, the effects of the DFT exchange-correlation operator are included in the MO eigenvectors and eigenvalues as a result of diagonalizing the KS matrix.

To proceed on to the SAPT part of the calculation, one then uses the 1- and 2-electron AO integrals, transforming them to integrals over MOs using the MO eigenvectors obtained from either the HF or KS equations. Finally, the excitation energies needed in the denominator of the second-order terms in the SAPT expansion of the interaction energy are obtained from the differences between MO eigenvalues, obtained through either the HF equations or the KS equations. In summary, the difference between the HF based SAPT versus the DFT based SAPT equations is the source of the MO eigenvectors and eigenvalues; in the former case these are calculated using the HF operator, and in the latter case they arise from application of the KS operator.

Some comments are in order concerning the use of KS MO eigenvectors and eigenvalues in this type of "sum over states" (SOS) perturbation approach. HF theory relates the eigenvalues to the ionization potentials of the electrons via Koopman's theorem.[47] In the KS implementation of DFT, the eigenvalues unfortunately do not have this simple intuitive meaning. Rather, DFT eigenvalues are related to the derivative of the energy with respect to orbital occupation number as shown by Janak.[48] The physical interpretation of the MO eigenvalues in DFT is made even more nebulous by the use of hybrid functionals such as Becke's three-term exchange functional, which contains some exact Hartree−Fock exchange.[52−54] Besides the basic difference in the physical content of the eigenvalues, there is another possible source of problems when using eigenvalues from a DFT calculation as first shown by Perdew and Levy.[49] The energy gaps between the occupied and unoccupied orbitals are underestimated due to the approximate form of the XC functionals. Specifically, the functionals do not have particle-number derivative discontinuities at integer particle values,[18,19,49] which is also partially responsible for an incorrect asymptotic behavior in the potential as one moves away from the atomic centers.[18,19] Any underestimation of the eigenvalue differences between HOMOs and LUMOs would lead to an overestimation in any interaction energy terms with energy denominators constructed from these MO eigenvalue differences, such as the second-order interaction energy terms in V seen in eq 12 (see ref 14, eqs 1.26 and 1.27, for the explicit form of the energy terms). In the case of the DFT-based SAPT approach being presented here, this would produce values for $E_{\text{disp}}^{(2)}$, $E_{\text{ind}}^{(2)}$, $E_{\text{exch-disp}}^{(2)}$, and $E_{\text{exch-ind}}^{(2)}$ in eq 19 that are larger than their correct values.

The use of canonical KS DFT MO eigenvectors and eigenvalues in a "sum over states" perturbation calculation has been studied previously to predict nuclear magnetic resonance (NMR) shielding tensors by Malkin, Malkina, Casida, and Salahub (MMCS).[16] Because SAPT also contains perturbation terms in an SOS representation, it is worth examining the quality of the results obtained by MMCS. The perturbation operator used in

calculating the NMR shielding tensors is a one-electron operator, whereas SAPT contains both one- and two-electron perturbation operators, but both have terms in the perturbation energy expansion that contain energy differences, $\Delta E_{k\rightarrow a}$, in their denominators. More specifically, in both cases these energy differences are represented as MO eigenvalue differences between filled ("k") and virtual ("a") KS MOs. In MMCS's work, they acknowledge the underestimation of the energy differences between HOMO−LUMO eigenvalues, and propose several approximations to correct these energy differences. Their simplest approximation is referred to as a "zeroth-order" approximation, i.e., $\Delta E_{k\rightarrow a} = e_k - e_a$, which uses the canonical KS MO eigenvalues, e_k and e_a, as is done in this study. They show that for many of the molecules tested, the NMR shielding tensors calculated with this zeroth-order $\Delta E_{k\rightarrow a}$ approximation are in good agreement with experiment. There are, however, NMR shielding tensors associated with certain atoms for which this simple approximation seems to fail, particularly with respect to quantitative predictions, and these tend to be atoms with multiple bonds, or pathological cases such as F_2.

The authors suggested two analytical forms for a correction term, $\Delta E^{XC}_{k\rightarrow a}$, to improve the approximation to the electronic transition energy according to $-\Delta E_{k\rightarrow a} = e_k - e_a - \Delta E^{XC}_{k\rightarrow a}$. This correction term accounts for part of the change in the exchange-correlation energy resulting from the transfer of an electron from MO "k" into MO "a". The use of this correction term (both forms) did indeed improve agreement between their calculated and the experimental NMR shielding constants.[16] However, even for problem cases such as PN, CO, F_2, N_2, and H_2CO, their calculations (using the zeroth-order $\Delta E_{k\rightarrow a}$ approximation) typically predicted correct trends in the relative magnitudes for the NMR coupling constants. MMCS's work seems to suggest that the canonical KS MO eigenvectors and eigenvalues represent a reasonable first approximation for defining the matrix elements and energy differences found in the individual SAPT terms.

A second point that needs to be emphasized is that within the KS part of the DFT-based SAPT calculation, monomers A and B are treated as isolated, noninteracting molecules. Hence, the electron density calculated via DFT for molecule A (or B) has no sense of the presence of its neighbor B(or A). The presence of monomer B is felt by A only through the SAPT interaction operator V as described in Section III.B. This is an important point because it guarantees that the DFT-SAPT approach does NOT "double-count" the correlation corrections to the intermolecular interaction energy.

Returning now to the specifics of combining DFT with SAPT, consider repartitioning the monomer SAPT Hamiltonian as $H_A = K_A$, where $K_A = T_0 + V_{eff}$ is a Kohn−Sham style operator. The operator will be defined similarly for monomer *B*. No operator analogous to W_A in the partitioning of Section III.B is defined here because the intramonomer electron correlation will be taken into account by our choice of V_{XC}. Then the new SAPT Hamiltonian would be $H = K + V$, where $K = K_A + K_B$ is the sum of the monomer operators and V is the intermolecular interaction operator, which is identical to the same operator presented in Section III.B. The interaction energy can now be expanded in a perturbation series in orders of V only, and is given by

$$E_{int}[XC] = E^{(1)}_{elst} + E^{(1)}_{exch} + E^{(2)}_{disp} + E^{(2)}_{ind} + E^{(2)}_{exch-disp} + E^{(2)}_{exch-ind} \quad (19)$$

where the parenthetical XC indicates that the approximation is dependent on a specific choice of the exchange-correlation functional. For emphasis we note that eq 19 contains only one perturbation index as compared to the two indices in eq 12, since no expansion in W is done to account for the intramolecular correlation, which is taken care of by the DFT correlation functional. Therein lies the motivation for combining these two theories, specifically, using DFT to replace the computationally demanding MBPT treatment of the intramolecular correlation corrections in SAPT. The abbreviation SAPT(DFT) will be used to indicate when density functional theory, as opposed to HF theory, is used as a starting point for SAPT.

IV. Computational Details

All calculations were performed with Gaussian 94[50] interfaced to the SAPT suite of codes.[51] Several combinations of DFT exchange-correlation functionals were tested in this study, and all are present in the Gaussian 94 library of functionals. They include the hybrid Becke-3 Lee−Yang−Parr (abbreviated B3LYP) functionals,[52] which contain the exchange contribution as a weighted sum of the exact HF exchange, the Slater (S) or local spin density (LSD) exchange,[53] and the Becke 88 functional (B),[54] which is itself a combination of the LSD exchange and a correction term involving the gradient of the density. The correlation functional in B3LYP is also a weighted sum of two terms, the LSD Vosko−Wilk−Nusair (VWN)[55] and the gradient-corrected Lee−Yang−Parr (LYP)[56,57] correlation functional. The other correlation functional used here is the gradient-corrected Perdew−Wang 91 (PW91).[58] The resulting combinations of exchange-correlation functionals tested include B3LYP, BLYP, SLYP, and BPW91. Finally, for the sake of comparison with a widely used method, second-order Moeller−Plesset (MP2) supermolecular calculations[50] were performed, with a frozen core, for most of the dimer systems at selected geometries. The MP2 results are included in the tables. The Boys−Bernardi[29] basis set superposition error corrections were included for these MP2 calculations.

The details concerning the atomic orbital basis sets used here can be found in Table 1. The *5*d and *7*f representations of the Gaussian functions were always selected. Both of the HF-based SAPT approaches, i.e., the benchmark SAPT and the approximate SAPT(HF), applied to the $(CO_2)-X$ systems, use the so-called monomer-centered plus basis sets (MC^+BS), which differ from the systems previously described wherein the full dimer-centered basis sets (DCBS) were used (excepting the He_2 system, which uses MC^+BS). The "plus" indicates the addition of functions beyond those assigned to the atoms in each monomer. For the sake of clarity, let us define a dimer system in which the first monomer is labeled A and the second as the "ghost monomer", with the goal of calculating molecular orbitals for A. One efficient way to allocate additional basis functions within the MC^+BS framework involves retaining the full atomic orbital basis set on monomer A, but only a subset of the full basis on the ghost monomer. A simple subset that produces good results is the original ghost monomer's basis less the higher angular momentum (i.e., polarization) functions. For example, if a 4s2p1d basis set is used for oxygen in the ghost monomer, then only the 4s2p portion would be retained at the oxygen position in the ghost monomer. For some dimer systems the MC^+BS also contains additional basis functions at the midbond location between the two monomers, as indicated in Table 1. This was done to improve the accuracy of the $E^{(20)}_{disp}$ term, which is variational in nature. In standard SAPT computations, the MC^+BS allocation substantially reduces the computational costs of the most time-consuming perturbational components, which

TABLE 1: Basis Sets Used in This Study, with References to Previous Caculations on Each System

system	ref	basis set label	basis composition	function location
He_2	25, 26	Dc147	7s5p4d3f/3s2p1d1f	He/midbond
Ar_2	20	"A"	7s4p2d1f	Ar
$(H_2O)_2$	15	D(d,p)*	4s2p1d/2s1p	O/H
		T^-(2d,2p)*	5s3p2d/3s2p	O/H
$(HF)_2$	15	D(d,p)′	4s2p1d/2s1p	F/H
		T^{-S}(2df,2pd)†	5s3p2d1f/3s2p1d	F/H
$Ar-H_2$	20	"A"	7s4p2d1f/3s2p	Ar/H
CO_2-CH_3CN	59, 61−63	Aug-cc- pVDZ	4s3p2d/4s3p2d/4s3p2d/3s2p	C/N/O/H
			2s2p2d1f1g	midbond[a]
CO_2−DMNA	60, 61−63	cc-pVDZ	3s2p1d/3s2p1d/3s2p1d/2s1p	C/N/O/H
			3s2p1d	midbond[a]

[a] Midbond functions were added exclusively in the calculation of the $E_{disp}^{(20)}$ [HF] term, and not in the SAPT(DFT) calculations. See text, section IV, and the references in this table for further clarification.

include intramonomer electron correlation. For example, the most time-consuming SAPT component, the triples contribution to $E_{disp}^{(22)}$, scales computationally as the fourth power of the number of virtual basis functions. The MC$^+$BS approach allows a 15−30% reduction in the basis size with almost no change in accuracy, resulting in an 3−6-fold reduction in the computational cost of this component. More details about this methodology and a description of its performance can be found in ref 23.

All SAPT(DFT) computations use the full DCBS. Although we would expect the MC$^+$BS method to work equally well, we have not yet performed adequate testing to ensure this. Because terms such as $E_{disp}^{(22)}$ are not computed in SAPT(DFT), the major computational advantage resulting from the use of MC$^+$BS, that is, the reduction in the number of virtual orbitals, would be lost. In principle, comparing computations between standard SAPT computations using a MC$^+$BS and SAPT(DFT) computations using a DCBS introduces another variable in the comparisons. In practice, however, it has been shown that the numerical results for standard SAPT computations using both the DCBS and MC$^+$BS are very close[23] to one another. Therefore, any uncertainty introduced into the comparison by this difference should be well below other sources of error in the present work.

He_2 [25,26] and Ar_2 [20] are two of the systems selected as prototypes for investigating the effects of using DFT as a starting point for SAPT, as benchmarks have already been reported for both of the systems. In He_2, the SAPT components included full intramonomer electron correlation (within the limits of the atomic orbital basis set) at the first- and second-order (in V) levels of theory. Single-point calculations were also performed for some selected systems for which there are already high-level SAPT calculations available. These include $(H_2O)_2$, $(HF)_2$, $Ar-H_2$, CH_3CN-CO, and dimethylnitramine−CO. The complete description of the geometries and computational details for $(H_2O)_2$ and $(HF)_2$ are detailed in ref 15, and for $Ar-H_2$ in refs 15 and 20. Finally, the two systems CH_3CN-CO and dimethylnitramine−CO (DMNA−CO) have been selected to study the interactions for larger molecules, which really provide the motivation for this work. The full monomer geometries and additional computational details are given in refs 59 and 60, respectively. It must be pointed out that for the largest system studied, i.e., DMNA$-CO_2$, and only for this system, the $E_{disp}^{(22)}$ term has not been calculated due to computational limitations.

V. Results and Discussions

As will be seen in the following results, there are clear trends in the interaction energies calculated with the new hybrid SAPT(DFT) approach that are present in most of the dimer systems. Therefore, only some systems will be analyzed in detail. The tables contain the interaction energy data, both the total interaction energies and the components, for all the systems studied to give the interested reader more details concerning the behavior of the approach with regards to specific types of atoms and molecules.

A. He_2. The helium dimer is the prototypical test system for weak intermolecular interactions because it is sufficiently small to make computations at the highest level of theory possible. References 25 and 26 investigated this system and provided SAPT benchmark results. Table 2 shows SAPT interaction energies calculated according to the three different approaches described in sections III.B and D. The benchmark results are the high-level SAPT results, including full intramonomer electron correlation, as described in section IV. These are represented by the components labeled $E^{(1)}$ and $E^{(2)}$ as defined by eq 11, and having only one superscript perturbation-order index that refers to the expansion in V. The total benchmark SAPT energy is merely the sum of these components, i.e., $E^{(1)} + E^{(2)}$. Except for $R = 5.6$ bohr, the benchmark values are previously unpublished results from refs 25 and 26. In the other two approaches, each of the SAPT components (and total interaction energy) was computed using either HF or DFT orbitals from eqs 12 or 19, respectively. Nine values of R were selected to indicate the performance of the method over the entire potential energy curve. The popular functional B3LYP was selected for these initial calculations. The sums of the SAPT components for these three implementations of SAPT are then plotted in Figure 1. In addition to the three SAPT approaches, the supermolecular DFT and HF results are plotted and labeled with the superscript "SM".

The supermolecular DFT and HF methods incorrectly predict the system to be unbound. This is no surprise for the HF interaction, where dispersion is nonexistent. In the case of the DFT results, this incorrect behavior results presumably from the inability of the current DFT exchange-correlation functional to adequately describe the dispersion interaction energy.[6−9,31] SAPT naturally includes the dispersion energy as a result of the computation. In this respect, it is a better approximation than the original Gordon and Kim[32] and Radzio-Andzelm and Kolos[34−36] approaches, which do not consistently include effects to second-order in the intermolecular interaction operator (V).

The SAPT(DFT) formulation does indeed correctly predict the He_2 to be bound, although the E_{int}^{SAPT}[B3LYP] curve has too shallow a well depth and its minimum is shifted to a larger interatomic separation. The SAPT(HF), i.e., E_{int}^{SAPT}[0], curve seems to have roughly the same structure as the benchmark curve but is even more weakly bound than the SAPT(DFT). The individual SAPT components for He_2 given in Table 2 have

TABLE 2: SAPT Components for He_2: A Comparison between Full Intramonomer Electron Correlation Results from Ref 26 (second entry in each component group) and Those of SAPT(HF)[a] and SAPT(DFT), in Rows One and Three in Each Group, Respectively[b]

R	3.0	4.0	4.5	5.0	5.3	5.6	6.0	6.5	7.0
$E_{elst}^{(10)}$ [a]	−1033.22	−89.37	−25.54	−7.21	−3.36	−1.56	−0.56	−0.15	−0.04
$E_{elst}^{(1)}$	−1065.50	−94.47	−27.33	−7.81	−3.67	−1.72	−0.62	−0.17	−0.05
$E_{elst}^{(1)}$ [B3LYP]	−1206.56	−122.20	−38.06	−11.77	−5.80	−2.86	−1.11	−0.34	−0.10
$E_{exch}^{(10)}$	5813.63	554.23	166.43	49.26	23.59	11.25	4.17	1.20	0.34
$E_{exch}^{(1)}$	6079.13	586.89	178.02	53.27	25.68	12.33	4.61	1.34	0.39
$E_{exch}^{(1)}$ [B3LYP]	7062.12	789.54	259.24	84.43	42.94	21.80	8.81	2.83	0.91
$E_{ind,resp}^{(20)}$	−415.04	−23.62	−5.68	−1.37	−0.59	−0.25	−0.08	−0.02	−0.01
$E_{ind}^{(2)}$	−437.86	−25.47	−6.19	−1.56	−0.65	−0.28	−0.09	−0.02	−0.01
$E_{ind}^{(2)}$ [B3LYP]	−520.33	−35.77	−9.54	−2.58	−1.18	−0.55	−0.20	−0.05	−0.02
$E_{disp}^{(20)}$	−765.98	−154.93	−73.60	−36.69	−24.78	−17.07	−10.69	−6.24	−3.82
$E_{disp}^{(2)}$	−927.70	−195.63	−94.33	−47.53	−32.24	−22.28	−14.00	−8.18	−5.01
$E_{disp}^{(2)}$ [B3LYP]	−1065.71	−231.03	−112.90	−57.47	−39.16	−27.14	−17.09	−9.99	−6.10
$E_{exch-ind,resp}^{(20)}$	361.42	20.70	4.88	1.16	0.49	0.21	0.07	0.02	0.00
$E_{exch-ind}^{(20)}$ [c]	420.53	24.11	5.77	1.39	0.59	0.25	0.08	0.02	0.01
$E_{exch-ind}^{(2)}$ [B3LYP]	469.12	33.05	8.73	2.34	1.07	0.49	0.17	0.05	0.01
$E_{exch-disp}^{(20)}$	110.31	16.20	5.66	1.92	0.99	0.51	0.21	0.07	0.02
$E_{exch-disp}^{(2)}$	198.19	23.07	7.89	2.67	1.38	0.72	0.29	0.10	0.03
$E_{exch-disp}^{(2)}$ [B3LYP]	149.46	25.76	9.78	3.61	1.97	1.06	0.47	0.16	0.06
E_{int}^{SAPT} [0]	4071.12	323.20	72.15	7.06	−3.66	−6.91	−6.89	−5.14	−3.50
$E^{(1)} + E^{(2)}$	4266.79	318.50	63.83	0.48	−8.91	−10.98	−9.72	−6.93	−4.64
E_{int}^{SAPT} [B3LYP]	4888.10	459.36	117.26	18.56	−0.18	−7.19	−8.95	−7.35	−5.24
E_{int}^{SM} [HF]	4268.45	428.79	131.54	39.64	19.16	9.22	3.45	1.00	0.29
E_{int}^{SM} [B3LYP]	3835.14	339.01	102.81	40.23	27.82	21.44	16.18	11.23	7.32

[a] To simplify the table, the label "HF" has been omitted from the interaction energy symbol. [b] Energies in units of Kelvin (1 a.u. = 315773 K) and distances are in bohr. [c] Only double exchanges are included; the so-called S^2 approximation.

been plotted in Figures 2a and 2b. To show the values from the entire potential energy surface, the logarithm of the individual values have been used. Figure 2a shows the negative of the attractive components and 2b shows the repulsive components. In general, the SAPT(DFT) results consistently differ more from the benchmark values than the results which start from HF theory. The second-order components ($E_{disp}^{(2)}$[B3LYP], $E_{ind}^{(2)}$[B3LYP], and their exchange counterparts) seem to consistently overshoot the benchmark values. This is the first example of how the under-estimated HOMO−LUMO energy gap adversely affects the second-order terms as discussed in section II.D. Because the total interaction energy given by E_{ind}^{SAPT}[B3LYP] differs less from the benchmark results than do the individual components, some cancellation of errors occurs.

The first-order terms in Table 2 raise an interesting question concerning the accuracy of the electron density predicted using B3LYP as one moves away from the He nucleus. Looking specifically at $R = 5.6$ au (3.0 Å), which is near the minimum energy, the first-order SAPT(HF) components are seen to be in better agreement with the benchmark values than the first-order components of SAPT(DFT). The first-order exchange is seen to be the largest destabilizing contribution to the total interaction energy, with the benchmark value given as 12.33 K. The value obtained for $E_{exch}^{(1)}$[B3LYP] is 21.80 K, nearly twice the magnitude of the benchmark value. In contrast, the energy obtained from $E_{exch}^{(10)}$[HF] is 11.25 K, in good agreement with the benchmark. This is of particular interest because the first-order components to the interaction energy, both the electrostatic and exchange, involve only electron densities (or more precisely, MO eigenvectors based on these densities) for systems A and B, and no energy denominators containing differences between orbital energies [see ref 30, eqs 6, 8, 9 for $E_{elst}^{(1)}$; and eqs 54−58 for $E_{exch}^{(1)}$]. Hence, for this somewhat large internuclear separation, one must conclude that the differences seen in Table 2 between the first-order interaction energies calculated from HF orbitals versus KS orbitals must be related to differences in the orbitals (and hence electron densities) themselves. This implies that the electron density obtained from B3LYP is a poorer description of the actual electron density than what one obtains from HF theory as one moves away from the nucleus to distances greater than the length of a typical covalent bond between two first row atoms, e.g., $R > 2.5$ Å.

We also tested other typical exchange-correlation functionals on the helium dimer system. For these functionals, only the distances $R = 4$, 5.6, and 7 bohr were investigated and the results are displayed in Table 3. The B3LYP functional gave as good or better agreement with the benchmark values for all the energy components at each value of R. B3LYP also performed better for the total interaction energy at each value of R, with one exception. The final value of E_{int} at $R = 4$ bohr is closer to the benchmark value when using the BLYP functional, but this is due to cancellation of errors as each of the components favors the B3LYP functional. Because this holds true for both the first- and second-order SAPT components, we will choose B3LYP to investigate the remaining dimer systems.

B. Ar_2. The argon dimer should provide a good many-electron test on a system dominated by dispersion energy. Table 4 contains the data for five distances ($R = 5$, 6, 7, 8, and 9 bohr).

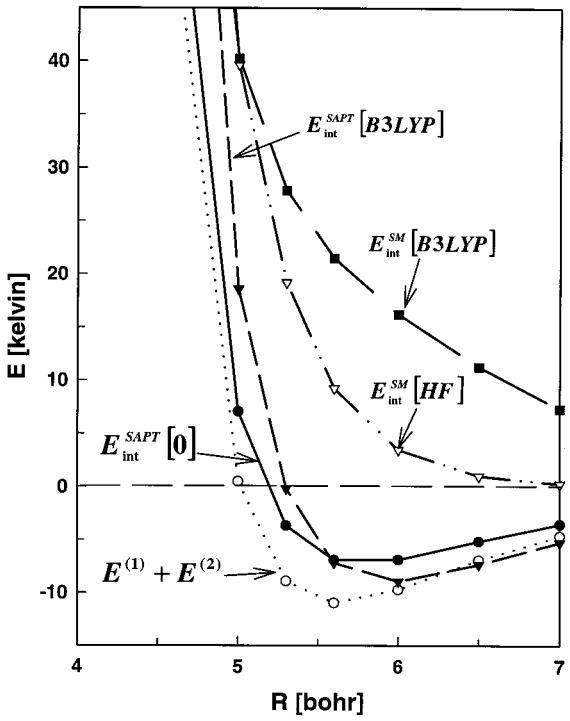

Figure 1. Comparison of the total interaction energy for He_2 calculated using various approximations. The dotted line with open circles are SAPT benchmark results from $E^{(1)} + E^{(2)}$ with full inclusion of intramonomer electron correlation. The solid line and circles indicate the SAPT(HF) in eq 12, and the long dashed line with solid triangles indicates the SAPT(DFT) in eq 19 using the B3LYP functionals. The dotted-dashed line with open triangles indicates the supermolecular HF energy, and the long-dashed line with solid squares indicates the supermolecular DFT results.

Results, which take into account full intramonomer correlation, are not available for this system. However, high level benchmark SAPT calculations have been performed according to eq 11. Most of the trends seen in the helium dimer results are present in these Ar_2 results. In the first-order terms, the SAPT(HF) underestimates the standard SAPT benchmark values, while the SAPT(DFT) overestimates these components. And the same trend exists in the second-order terms, wherein the SAPT(DFT) components overestimate the benchmark values and SAPT(HF) underestimates them. At $R = 7.0$ bohr (near the energy minimum), the total interaction energy from SAPT(HF) is -118 K, which is close to but slightly below the benchmark SAPT value of -110 K. This is the reverse of what was seen in He_2 where the SAPT(HF) total interaction energy underestimated the benchmark SAPT value. The SAPT(DFT) total interaction energy at this same point is calculated to be -206 K, which puts it nearly a factor of 2 below the SAPT benchmark value. Table 4 also includes the MP2 interaction energy of -104 K at $R = 7.0$ bohr, which is in better agreement with the benchmark value of -110 than either the SAPT(HF) or SAPT(DFT) result.

These trends are clearly discernible in Figure 3, which contains plots of the potential energy curves for four approximations to the total interaction energy, and compares them to the SAPT benchmark curve. The four theoretical curves represent the two SAPT approximations, SAPT(DFT) and SAPT(HF), and supermolecular B3LYP and HF results. The main message contained in Figure 3 is that both SAPT methods show significant binding, with minima in the vicinity of the benchmark minimum, while the supermolecular approaches show no binding at all. This is just another example of the potential power of this new hybrid SAPT(DFT) method to calculate dispersive interactions in systems where supermolecular DFT might fail.

C. Ar−H_2. Moving away from the noble gas dimers, the results from a selection of other systems are displayed in Table 5. The first system, Ar−H_2, is a prototype noble gas/molecule interaction. The dispersion energy is as important for this system as for the previous two systems. There are two stable conformations predicted by the benchmark SAPT calculations, referred to in Table 5 as Linear and T-shape (with the meanings of the labels being self-evident). In both cases, the inter-monomer separation (centers-of-mass) is ~3.6 Å. Once again, the supermolecular B3LYP and HF results fail to predict that the system is bound for either conformation, whereas all three implementations of SAPT predict both the Linear and T-shape to be bound. In addition, SAPT(DFT) predicts the correct order for the total binding energy between the two conformers. The benchmark values for the total binding energy are -121 and -85 cal/mol in the Linear and T-shape, respectively. The corresponding SAPT(DFT) values are -189 and -128 cal/mol, respectively. The SAPT(HF) values also predict the correct trend, and in better agreement with the benchmark values, with energies of -95 and -67 cal/mol, respectively. The MP2 interaction energies are -93 and -63 cal/mol, which are very close to the SAPT(HF) values.

Again, one noteworthy observation is that the SAPT(DFT) first-order terms are in relatively poor agreement with the benchmark values. For the linear geometry, the $E_{elst}^{(1)}$[B3LYP] and $E_{exch}^{(1)}$[B3LYP] are 24% and 23% too large compared to the benchmark, and for the T-shape geometry they are 22% and 23% too large, respectively. The first-order terms from the SAPT(HF) approximation are in much better agreement with the benchmark values, differing by no more than 8%. As in He_2, this would suggest that (at least) the outer regions of the electron densities for the monomers derived from HF theory are better approximations to the zeroth-order densities than what are obtained from the DFT. The general trends in total energies and the remaining components are similar to those seen in the Ar_2, so no additional detailed analysis will be given.

D. $(H_2O)_2$ and $(HF)_2$. The next two systems, $(H_2O)_2$ and $(HF)_2$, contain permanent electric dipole moments, unlike the previously described systems. Thus, the first-order components, particularly the electrostatic energy, should make a significant contribution to the final interaction energy. This is supported by the results in Table 5 where it is seen that the first-order electrostatic interaction energies are the largest contributors to the total interaction energies, and are 3−5 times larger than the dispersion contributions. Another contrast with the previous dimer systems is the supermolecular B3LYP total interaction energy, which not only predicts binding but is in good agreement with the SAPT benchmark result for both dimers. The E_{int}^{SM}[B3LYP] values differ from the benchmark values by only 12% and 16% for the larger basis set in $(H_2O)_2$ and $(HF)_2$, respectively. It is encouraging to note that in both dimer systems, particularly with the larger basis set, the first-order components from SAPT(DFT) compare well with the benchmark $E_{elst}^{(1)}$ (3) and $E_{exch}^{(1)}$ (3), and are in better agreement with the benchmark results than the SAPT(HF) energies. This is the reverse of what was observed in the previous dimer systems, indicating that in strongly polar molecules, the electron density from the B3LYP functionals provides a good zeroth-order wave function for use in the SAPT procedure.

Finally, following previous trends, SAPT(DFT) again overestimates the second-order terms. However, because the stabilizing interactions are dominated more by the electrostatic rather than the dispersive interactions, the effect of this overestimation

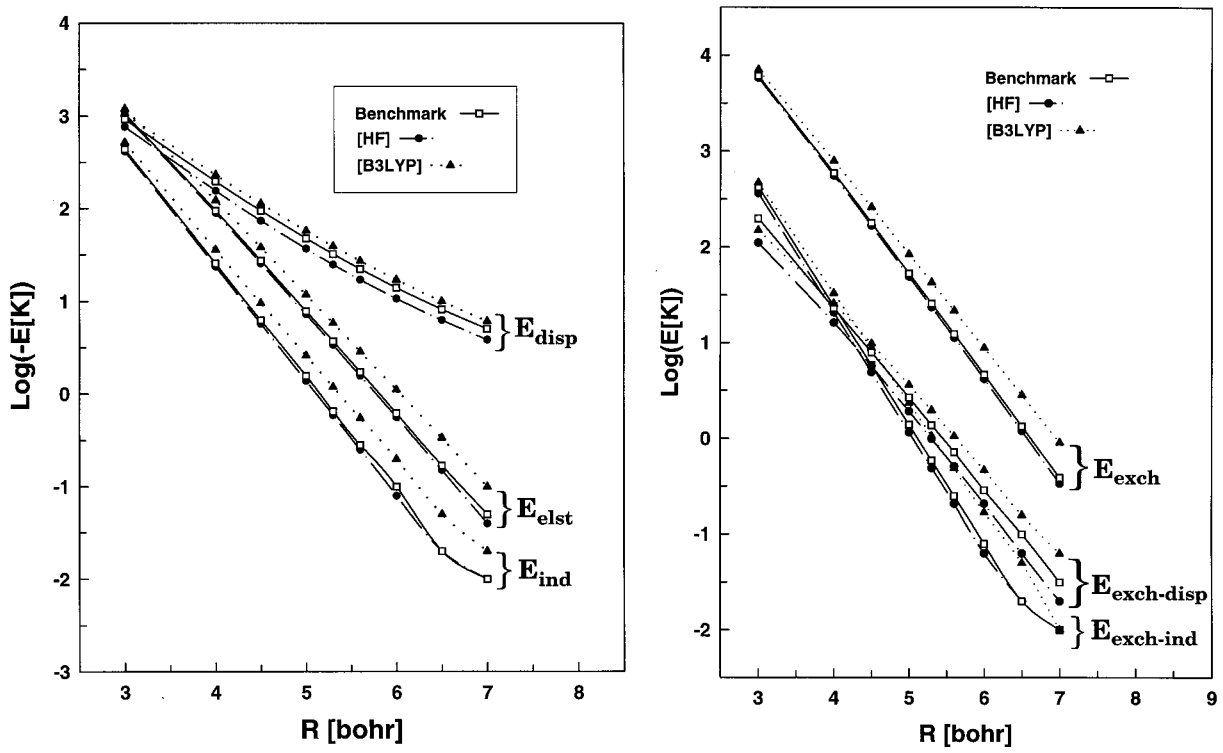

Figure 2. The benchmark SAPT interaction energies for each component are displayed with solid lines and open squares; the dashed−dotted lines with solid circles indicate the SAPT(HF), eq 12; and the dotted lines with solid triangles indicate the SAPT(DFT) results, eq 19. All data is taken from Table 2. (a) The attractive components of the He_2 interaction energies. The vertical scale is the logarithm of the negative of the energy in order to display the entire range of the values. (b) The repulsive components of the He_2 interaction energies.

in the dispersion term has only a minor effect on the total SAPT-(DFT) interaction energies, which now actually underestimate the benchmark values. It is interesting to note that the discrepancy between the SAPT(DFT) and benchmark total interaction energies is about equal to the correction term δE_{int}^{HF} from eq 8. As a reminder, this is the correction to the interaction energy for higher-order induction and exchange-induction terms not included in the SAPT implementation, but present in the HF supermolecular interaction energy. This values does get included in the total benchmark interaction energy, but no analogous correction for such higher-order terms is included in the SAPT-(DFT) total interaction energy. It is not obvious how one would go about estimating these contributions in a similar fashion for DFT based calculations. However, if the δE_{int}^{HF} in Table 5 can be considered a reasonable estimate for these terms in the SAPT-(DFT) implementation (since it includes only induction and exchange corrections), and if it were to be included in the SAPT-(DFT) total interaction energies, the agreement with the benchmark values would be remarkably good. For example, in $(H_2O)_2$ with the larger basis set, adding this estimate of higher-order corrections gives $E_{int}^{SAPT}[B3LYP] + \delta E_{int}^{HF} = -4.58$ kcal/mol, as compared to −4.49 kcal/mol for the benchmark value: A difference of only 2%.

E. CH_3CN-CO_2 and DMNA−CO_2. CH_3CN-CO_2 is the first of two dimer systems selected to provide tests for the performance of the method for larger molecular systems. In this study, the CH_3CN-CO_2 dimer is the largest system that includes all of the MBPT terms for the intramolecular correlation corrections typically used in the standard SAPT implementation. Therefore, it is worth examining the computational savings that result from using this new hybrid method on this dimer. The CPU time required for a single processor calculation on $CH_3-CN-CO_2$ (one conformation) using the conventional SAPT implementation, referred to as the "benchmark" calculation, was ∼243 000 CPU seconds. The same calculation using the SAPT-(DFT) approach required only ∼1900 CPU seconds. This huge difference in CPU times is not surprising, as terms such as the second-order $E_{disp}^{(22)}$ scale according to $n^3(N^4) + n^4(N^3)$, where "n" are the filled orbitals and "N" the virtual orbitals, while $E_{disp}^{(20)}$ scales as $n^2(N^2)$. Quite simply, replacing the MBPT intramonomer correlation treatment by a DFT approach has drastically reduced the computational time *by a factor of 128*! This tremendous savings certainly justifies the examination of such a hybrid method.

The results for CH_3CN-CO_2 are presented in Table 5 for two minimum energy conformations, labeled G1 and G2, and for a local minimum on the DMNA−CO_2 potential energy surface. G1 corresponds to a structure with the lowest energy found on the CH_3CN-CO_2 potential energy surface. Once again, the SAPT(DFT) method predicts the correct relative interaction energies between the two conformations G1 and G2. Unlike the $(H_2O)_2$ and $(HF)_2$ cases, in these two systems the electrostatic and dispersive interactions are approximately of the same magnitude, so that the overestimation of the dispersive terms once again contributes to the SAPT(DFT) overestimating the total interaction energies of G1(−3.79 kcal/mol) and G2(−1.60 kcal/mol) when compared to the benchmark values of G1(−2.51 kcal/mol) and G2(−1.12 kcal/mol). The same trend can be seen for DMNA−CO_2, where the SAPT(DFT) and benchmark values are −3.34 and −2.02 kcal/mol. In the DMNA−CO_2 case, the discrepancy between the SAPT(DFT) and benchmark total interaction energies is somewhat misleading since, as mentioned in section IV, the benchmark calculations for this particular dimer do NOT contain the $E_{disp}^{(22)}$ component as in all other benchmark calculations. Previous numerical experience indicates[13] that this would probably lower the total benchmark result by 5%−20%. Whereas this would improve

TABLE 3: Comparison SAPT Components for the He_2 System Obtained Using DFT Theory as a Starting Point with Various Exchange-Correlation Functionals[a]

XC	BLYP[b]	BPW91[c]	SLYP[d]	B3LYP[e]	benchmark[f] $E^{(1)}+E^{(2)}$
			$R=4.0$		
$E^{(1)}_{elst}$	−135.95	−124.41	−162.59	−122.20	−94.97
$E^{(1)}_{exch}$	892.82	820.03	1050.56	789.54	586.89
$E^{(2)}_{ind}$	−43.16	−38.94	−53.97	−35.77	−25.47
$E^{(2)}_{disp}$	−262.85	−249.90	−301.53	−231.03	−195.63
$E^{(2)}_{exch-ind}$	41.79	37.55	51.97	33.05	24.11
$E^{(2)}_{exch-disp}$	29.95	27.75	35.46	25.76	23.07
E_{int}	522.60	472.08	619.90	459.35	318.00
			$R=5.6$		
$E^{(1)}_{elst}$	−3.55	−3.16	−4.54	−2.86	−1.72
$E^{(1)}_{exch}$	27.62	25.04	34.74	21.80	12.33
$E^{(2)}_{ind}$	−0.74	−0.67	−0.99	−0.55	−0.28
$E^{(2)}_{disp}$	−31.67	−29.84	−36.96	−27.14	−22.28
$E^{(2)}_{exch-ind}$	0.70	0.63	0.93	0.49	0.25
$E^{(2)}_{exch-disp}$	1.37	1.21	1.74	1.06	0.72
E_{int}	−6.27	−6.79	−5.08	−7.20	−10.98
			$R=7.0$		
$E^{(1)}_{elst}$	−0.14	−0.13	−0.20	−0.10	−0.05
$E^{(1)}_{exch}$	1.29	1.16	1.73	0.91	0.39
$E^{(2)}_{ind}$	−0.02	−0.02	−0.03	−0.02	−0.01
$E^{(2)}_{disp}$	−7.15	−6.74	−8.33	−6.10	−5.01
$E^{(2)}_{exch-ind}$	0.02	0.02	0.03	0.01	0.01
$E^{(2)}_{exch-disp}$	0.08	0.07	0.11	0.06	0.03
E_{int}	−5.92	−5.64	−6.69	−5.24	−4.64

[a] The basis sets are described in section IV. E_{int} sums the previous six components. The last two columns are excerpted from Table 2 for convenient comparison. Energies are in units of kelvin (1 a.u. = 315773 K) and distances in bohr. [b] See refs 54, 56, 57. [c] See refs 54 and 58. [d] Refs 53, 56, 57. [e] See ref 52. [f] Full intramonomer correlation (see ref 26 and text).

TABLE 4: SAPT Components Using HF and DFT Theory as Starting Points for Ar_2[a]

R	5	6	7	8	9
$E^{(10)}_{elst}$	−4064.85	−549.13	−72.47	−9.42	−1.20
$E^{(1)}_{elst}$ (3)	−4379.48	−618.23	−86.75	−12.43	−1.90
$E^{(1)}_{elst}$ [B3LYP]	−4540.19	−670.37	−97.67	−14.31	−2.13
$E^{(10)}_{exch}$	11885.85	1751.12	247.53	33.95	4.55
$E^{(1)}_{exch}$ (3)	12489.39	1905.46	278.26	39.39	5.44
$E^{(1)}_{exch}$ [B3LYP]	12907.99	2070.95	324.53	50.27	7.74
$E^{(20)}_{ind}$	−7099.55	−755.64	−81.15	−8.83	−0.96
$E^{(2)}_{ind}$ (2)[b]	−9368.23	−1000.78	−108.79	−12.16	−1.42
$E^{(2)}_{ind}$ [B3LYP]	−10105.91	−1181.42	−142.46	−17.78	−2.29
$E^{(20)}_{exch-ind}$	6686.91	735.39	79.32	8.61	0.93
$E^{(2)}_{exch-ind}$ (2)[c]	8894.33	981.13	106.85	11.89	1.38
$E^{(2)}_{exch-ind}$ [B3LYP]	9633.31	1163.00	140.79	17.54	2.25
$E^{(20)}_{disp}$	−2644.40	−871.83	−312.17	−124.01	−55.26
$E^{(2)}_{disp}$ (2)	−2569.91	−870.39	−311.66	−121.55	−52.95
$E^{(2)}_{disp}$ [B3LYP]	−3807.86	−1287.53	−468.33	−186.98	−83.09
$E^{(20)}_{exch-disp}$	581.94	117.73	21.12	3.47	0.52
$E^{(2)}_{exch-disp}$ [B3LYP]	873.81	188.28	36.68	6.61	1.10
E^{SAPT}_{int} [0][d]	5345.91	427.63	−117.82	−96.24	−51.41
$E^{SAPT\,f}_{int}$	5390.94	444.62	−109.86	−92.45	−49.05
E^{SAPT}_{int} [B3LYP][e]	4961.15	282.91	−206.46	−144.65	−76.42
E^{MP2}_{int}			−105.26		
E^{SM}_{int} [HF]	7134.22	1114.46	164.52	23.25	3.20
E^{SM}_{int} [B3LYP]	5985.16	813.56	98.15	34.37	26.20

[a] Energy components without brackets use the standard HF orbitals as a starting point. Distances are in bohr and energies in kelvin. [b] $E^{(2)}_{ind}(2) \equiv E^{(20)}_{ind,resp} + {}^tE^{(22)}_{ind}$ [c] $E^{(2)}_{exch-ind}(2) \equiv E^{(20)}_{exch-ind,resp} + {}^tE^{(22)}_{exch-ind}$ [d] Computed according to eq 12; SAPT(HF) with no intramonomer correlation. [e] Computed according to eq 19. [f] Computed according to eq 11; standard SAPT including intramonomer correlation and δE^{HF}_{int}.

the agreement between the SAPT(DFT) and the benchmark results, it would account for only one-third, at best, of the entire 1.3 kcal/mol difference which now separates the two total interaction energies.

The overestimation of the second-order terms is particularly exaggerated for the dispersion interaction energy, $E^{(2)}_{disp}$-[B3LYP], where one sees magnitudes of −5.06 and −2.08 kcal/mol for conformations G1 and G2, respectively. This is to be compared with the benchmark values of −3.28 and −1.36 kcal/mol, in that order. In contrast, the first-order electrostatic and exchange interactions, $E^{(1)}_{elst}$[B3LYP] and $E^{(1)}_{exch}$[B3LYP], for both CH_3CN-CO_2 and for $DMNA-CO_2$, are in much better agreement with the benchmark SAPT values, $E^{(1)}_{elst}$ (3) and $E^{(1)}_{exch}$ (3), than are the second-order components**.** The first-order SAPT(DFT) electrostatic terms differ from the benchmark results by only 3% and 6% for G1 and G2 respectively, whereas the exchange components differ by 8% and 17%, with the largest absolute discrepancy being 0.32 kcal/mol for the G1 exchange interaction energy. And the agreement is even better for $DMNA-CO_2$. Hence, it would appear that this new hybrid SAPT(DFT) method is capable of describing electrostatic interactions, e.g., hydrogen bonding, quite reliably in systems where this plays a major role.

There are some interesting observations that can be made if one examines the first- and second-order SAPT(DFT) components across Tables 2−5. There are at least three general statements that can be made: (i) The first-order terms from SAPT(DFT) show good agreement with the benchmark values in systems containing monomers that have permanent (sizable) electric dipole moments; (ii) the first-order electrostatic contributions tend to be in better agreement with the benchmark numbers than the first-order exchange contributions, and (iii) the second-order terms, and particularly the dispersion part of the interaction energy, always overestimate (and in some cases drastically overestimate) the benchmark values. The explanation for the behavior of the first-order terms, e.g., electrostatic versus exchange interactions, based on these data alone would be mostly conjecture, and hence, requires further study. However, the overestimation of the second-order terms is most likely related to the well-established underestimation of the HOMO−LUMO energy gap, as discussed in section III.D. This is a serious problem, but one which has been addressed with some success in the recent literature.

F. Improved Transition Energies for Use in Perturbation Theory. It was already mentioned in section III.D that MMCS[16] proposed and tested a method for improving the estimate of the excitation energy involved in a SOS perturbation term beyond what they called their "zeroth-order" approximation, which is analogous to the approximation used in this SAPT approach. While MMCS showed that their approach did indeed improve the prediction of NMR shielding constants, there has been other work aimed at improving estimates to the electronic

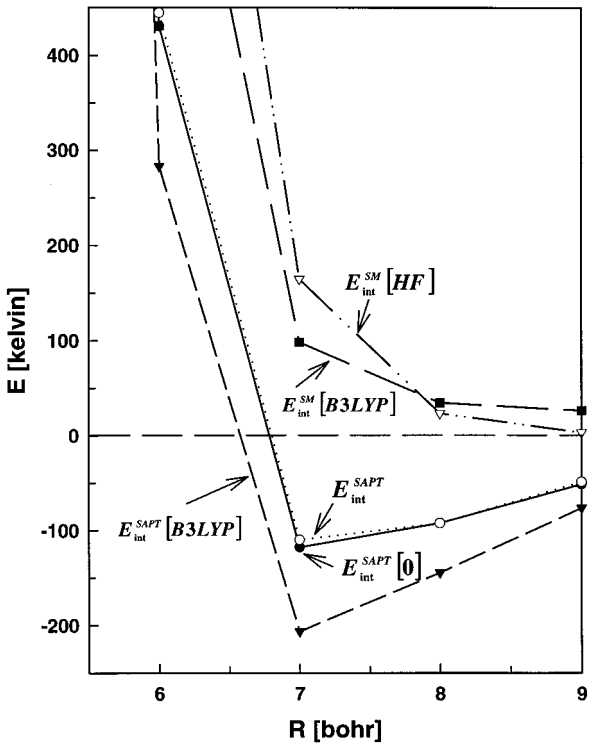

Figure 3. The total interaction energy for the Ar_2 system from the benchmark SAPT (dotted line/open circles) and SAPT(DFT) (shorter dashed line/downward solid triangles). The solid line/solid circles are the SAPT(HF) results. The supermolecular HF (dot−dashed line/open diamonds) and DFT (longer dashed line/solid squares) results are also displayed.

transition energy based upon energy differences between KS MO eigenvalues. Handy and co-workers[12,17−19] have worked with notable success in identifying the sources of the unphysically small energy gap between HOMOs and LUMOs calculated using popular exchange-correlation functionals. Their approach entails the development of new functionals designed explicitly with the goal in mind of "improving virtual Kohn−Sham orbitals and eigenvalues".[18] This work is based upon requiring the exchange-correlation potential to exhibit the correct asymptotic behavior, that is to say, functionals whose potential decays not to zero at infinity, but to a constant value related to the ionization energy and electron affinity of an atomic or molecular system. This is was shown to give energy differences between filled and virtual MOs that more closely represent electronic excitation energies in the hydrogen atom and a selection of test molecules.[18] It was also pointed out that functionals such as BLYP fail to reproduce this form of asymptotic behavior.[19] It is worth noting that the asymptotic behavior of the potential has little effect on the filled molecular orbitals and their eigenvalues, indicating the adequacy of existing functionals in describing the electron density near bonding regions, but can have a significant effect on the virtual orbitals.[19] Work is already underway to combine these new functionals[18] with SAPT, and test results will be forthcoming.

In another approach called the "optimized effective potential" (OEP) method,[64] the exchange-correlation potential, V_{XC}^{OEP}, is defined in terms of spin−orbitals. One can understand the significance of this orbital dependence if one demands that this V_{XC}^{OEP} potential be the one that contains orbitals that minimize the total energy of the system, implying that V_{XC}^{OEP} depends on some optimal set of molecular orbitals (in terms of energy). While it is clear that this approach will produce a set of optimized DFT *occupied* molecular orbitals, it is not clear whether this method could be used to improve the description of the virtual orbitals or their eigenvalues. Grabo et al.[64] do outline a means for combining the OEP method with many body perturbation theory, but no applications are presented. For the sake of completeness, it is worth mentioning other attempts to find the excitation energies from a DFT computation such as Slater's transition state concept[65] and generalization,[66] and more recent work by Levy.[67]

VI. Conclusions

This is the first attempt at a hybrid approach, utilizing popular DFT exchange-correlation functionals, for describing intermolecular interaction energies that includes, in a natural way, the van der Waals (dispersive) interactions. This method combines symmetry adapted perturbation theory along with Kohn−Sham DFT. Such a scheme should, in principle, eliminate the need to calculate the intramolecular (or intraatomic) correlation corrections using the computationally intensive many-body perturbation theory typically used in SAPT, as these "corrections" should be included in the DFT exchange-correlation functionals. This hybrid method has been labeled SAPT(DFT). It was shown that SAPT(DFT) gave qualitatively correct binding trends between conformers in all dimer systems, including those dominated by dispersive interactions where supermolecular DFT failed, while providing a tremendous reduction in computational time by a factor on the order of 10^2!

This initial implementation of SAPT(DFT) does fall short of the quantitative accuracy normally associated with correlated ab initio techniques for total interaction energies. However, through the SAPT energy decomposition at least two significant facts were revealed: (1) This new hybrid SAPT(DFT) method predicts electrostatic interactions in very good agreement with high-level ab initio calculations for systems containing polar molecules; and (2) much of the error in the SAPT(DFT) total interaction energies resided in the second-order terms, and particularly the dispersion terms, which consistently overestimated the benchmark values. This error in the second-order terms is attributed primarily to the use of canonical KS MO energies, e_k and e_a in $\Delta E_{k\rightarrow a} = e_k - e_a$, that is, the energy differences used in the denominators of the second-order interaction energy terms. As discussed in this paper, the energy separation between the filled and virtual orbitals is underestimated when obtained from some of the most widely used DFT exchange-correlation functionals. In contrast to the second-order terms, the SAPT(DFT) first-order terms, such as the electrostatic interaction energy, were seen to be in much better agreement with the benchmark values, particularly for systems containing polar monomers. These first-order terms depend only on the filled MO eigenvectors, which are a direct result of the electron density calculated for each monomer via DFT. This implies that the original ansatz of choosing DFT electron densities to produce zeroth-order wave functions for use in this hybrid SAPT scheme does indeed merit further exploration, assuming the virtual orbital eigenvalue problem can be resolved.

The SAPT decomposition of the total interaction energy into physically meaningful terms, e.g., electrostatic, dispersion, etc., is useful in itself in gaining an understanding of the forces holding together a molecular ensemble. In addition, this energy decomposition provides the opportunity to invert the thrust of the current study and utilize SAPT to "fine-tune" the fitting procedures used in the development of exchange-correlation functionals. Fitting to a single number like the experimental (or supermolecular) interaction energy when adjusting the parameters used to define exchange-correlation functionals

TABLE 5: Comparison of SAPT Components Using HF or DFT Theory as a Starting Point[a]

system [ref]	Ar−H_2 [20]		$(H_2O)_2$ [15]		$(HF)_2$ [15]		CH_3CN-CO_2 [59]		DMNA−CO_2 [60]
description	linear	T-shape	D(d,p)*	T^-(2d,2p)*	D(d,p)*	T^{-S}(2d,2p)†	G1	G2	$R = 4.8125$
$E_{elst}^{(10)}$	−76.1	−55.3	−7.41	−7.12	−6.99	−6.33	−3.64	−1.07	−3.03
$E_{elst}^{(1)}$ (3)	−81.4	−59.1	−7.36	−7.00	−6.71	−6.06	−3.10	−0.96	−2.97
$E_{elst}^{(1)}$ [B3LYP]	−101.1	−72.1	−7.44	−7.00	−6.85	−6.18	−3.19	−1.02	−3.01
$E_{exch}^{(10)}$	301.4	216.3	5.10	5.13	4.75	4.57	3.88	1.09	2.17
$E_{exch}^{(1)}$ (3)	327.2	231.3	6.40	6.31	6.18	5.82	4.14	1.29	2.92
$E_{exch}^{(1)}$ [B3LYP]	402.7	284.3	6.66	6.60	6.54	6.22	4.46	1.51	3.08
$E_{ind}^{(20)}$	−68.5	−41.5	−1.78	−1.79	−1.94	−2.00	−1.67	−0.23	−0.88
$E_{ind}^{(2)}$ (2)[b]	−79.6	−47.3	−2.68	−2.64	−2.93	−2.92	−2.00	−0.29	−1.41
$E_{ind}^{(2)}$ [B3LYP]	−115.9	−68.1	−2.99	−2.89	−3.22	−3.25	−2.26	−0.39	−1.75
$E_{exch-ind}^{(20)}$	59.7	39.6	0.95	0.93	1.00	0.92	1.24	0.12	0.62
$E_{exch-ind}^{(2)}$ (2)[c]	69.9	45.4	1.46	1.41	1.50	1.36	1.54	0.16	1.03
$E_{exch-ind}^{(2)}$ [B3LYP]	105.2	66.1	1.88	1.75	1.95	1.80	1.70	0.23	1.40
$E_{disp}^{(20)}$	−333.2	−241.7	−1.66	−1.85	−0.97	−1.49	−3.22	−1.26	−2.00
$E_{disp}^{(2)}$ (2)	−358.8	−262.3	−2.03	−2.24	−1.31	−1.90	−3.28	−1.36	−1.54
$E_{disp}^{(2)}$ [B3LYP]	−517.3	−363.0	−2.61	−2.95	−1.62	−2.40	−5.06	−2.08	−3.42
$E_{exch-disp}^{(20)}$	21.4	15.2	0.28	0.31	0.14	0.22	0.36	0.08	0.15
$E_{exch-disp}^{(2)}$ [B3LYP]	37.0	25.1	0.51	0.55	0.28	0.40	0.56	0.15	0.38
δE_{int}^{HF} [d]	−19.8	−8.6	−0.62	−0.64	−0.61	−0.61	−0.16	−0.06	−0.12
E_{int}^{SAPT} [0][e]	−95.3	−67.4	−4.52	−4.38	−4.01	−4.11	−3.04	−1.27	−2.95
E_{int}^{SAPT} [f]	−121.1	−85.4	−4.56	−4.49	−3.73	−4.08	−2.51	−1.12	−2.02
E_{int}^{SAPT} [B3LYP][g]	−189.5	−127.8	−3.99	−3.94	−2.93	−3.41	−3.79	−1.60	−3.34
E_{int}^{MP2}	−93.6	−62.9	−4.49	−4.40	−3.69	−4.00	−2.14	−0.91	−2.37
E_{int}^{SM} [HF]	195.9	150.6	−3.93	−3.65	−4.00	−3.66	−0.39	−0.15	−1.34
E_{int}^{SM} [B3LYP]	119.9	137.1	−4.74	−4.36	−4.52	−4.26	−0.43	−0.13	−1.26

[a] Dimer geometries are near a global or local minimum, and for the systems with a single geometry, the global minimum is chosen. Energy components without brackets use the HF orbitals as a starting point. $(H_2O)_2$ and $(HF)_2$ show data for two different basis sets (see Table 1). Energy units are cal/mol for Ar−H_2, and Kcal/mol for all others. [b] $E_{ind}^{(2)}$ (2) $\equiv E_{ind,resp}^{(20)} + {}^tE_{ind}^{(22)}$ [c] $E_{exch-ind}^{(2)}$ (2) $\equiv E_{exch-ind,resp}^{(20)} + {}^tE_{exch-ind}^{(22)}$ [d] From eq 8. Higher-order induction and exchange-induction interaction energies absent in current SAPT codes but present in supermolecular HF interaction energy. [e] From eq 12; SAPT(HF) with no intramonomer coorelation. [f] From eq 11; standard SAPT with intramonomer correlation and δE_{int}^{HF}. [g] From eq 19.

always includes the possibility of getting the right answer but for the wrong reasons, i.e., a cancellation of errors. SAPT could be used to provide a more fundamental understanding about the performance of these functionals in order to improve their performance in the prediction of the weaker intermolecular interactions, specifically, the dispersion and electrostatic energies.

This work further documented the claims that DFT, used in the typical supermolecular approach, fails to adequately predict intermolecular interactions dominated by dispersive interactions, at least with the functionals tested in this study. The supermolecular DFT approach predicted the dimers He_2, Ar_2, and Ar−H_2 to be unbound, which is known to be incorrect. However, supermolecular DFT did much better for describing intermolecular interactions between polar molecules where the stabilizing interaction energy components were dominated by the electrostatic terms rather that the dispersive terms, as was the case in $(H_2O)_2$ and $(HF)_2$.

The next step in this research is to test newly developed exchange-correlation functionals,[18,19] designed to specifically address the virtual orbital eigenvalue problem, and determine their ability to improve the quantitative accuracy for the second-order SAPT terms, while hopefully retaining or improving the accuracy of the first-order interaction terms. If such improvements are realized, the result will be a hybrid scheme capable of producing intermolecular interaction energies with accuracies approaching a high level correlated ab initio technique, but at a fraction of the computational costs, while retaining the benefits of the energy decomposition that occurs naturally through the use of symmetry adapted perturbation theory. Work is currently underway to implement a version of SAPT that uses these newer functionals, and data will be forthcoming.

Acknowledgment. This work was partially supported by the Strategic Environmental Research and Development Program (SERDP), Project PP-695. The authors gratefully acknowledge the computer resources made available for this study on the SGI Power Challenge Array by the DOD Major Shared Resource Center at the Army Research Laboratory (ARL), Aberdeen Proving Ground, MD. This research was performed while HW was a National Research Council postdoctoral associate at ARL and he wishes to thank both organizations for their support. The authors would also like to thank Krzysztof Szalewicz and Bogumil Jeziorski for reading and commenting on the manuscript.

References and Notes

(1) Hohenberg, P.; Kohn, W. *Phys. Rev. B* **1964**, *136*, 864.
(2) Kohn, W.; Sham, L. J. *Phys. Rev. A* **1965**, *140*, 1133.

(3) Parr, R. G.; Yang, W. *Density-Functional Theory of Atoms and Molecules*; Oxford University, New York, 1989.
(4) Ziegler, T. *Chem. Rev.* **1991**, *91*, 651.
(5) Parr, R. G.; Yang, W. *Annu. Rev. Phys. Chem.* **1995**, *46*, 701.
(6) Kristyan, S.; Pulay, P. *Chem. Phys. Lett.* **1994**, *229*, 175.
(7) Perez-Jorda, J. M.; Becke, A. D. *Chem. Phys. Lett*. **1995**, *233*, 134.
(8) Hobza, P.; Sponer, J.; Reschel, T. *J. Comput. Chem.* **1995**, *16*, 1315.
(9) Proynov, E. I.; Ruiz, E.; Vela, A.; Salahub, D. R. *Int. J. Quantum Chem.: Quantum Chem. Symp.* **1995**, *29*, 61.
(10) London, F. *Z. Phys.* **1930**, *63*, 245.
(11) Sponer, J.; Leszczynski, J.; Hobza, P. *J. Biomol. Struct. Dyn.* **1996**, *14*, 117.
(12) Boese, A. D.; Doltsinis, N. L.; Handy, N. C.; Sprik, M. *J. Chem. Phys.* **2000**, *112*, 1670.
(13) Jeziorski, B.; Moszynski, R.; Szalewicz, K. *Chem. Rev.* **1994**, *94*, 1887.
(14) Szalewicz, K.; Jeziorski, B. In *Molecular Interactions − From van der Waals to Strongly Bound Complexes*; Scheiner, S., Ed.; Wiley: New York, 1997; p. 3.
(15) Williams, H. L.; Szalewicz, K.; Moszynski, R.; Jeziorski, B. *J. Chem. Phys.* **1995**, *103*, 4586.
(16) Malkin, V. G.; Malkina, O. L.; Casida, M. E.; Salahub, D. R. *J. Am. Chem. Soc.* **1994**, *116*, 5898.
(17) Hamprecht, F. A.; Cohen, A. J.; Tozer, D. J.; Handy, N. C. *J. Chem. Phys*. **1998**, *109*, 6264.
(18) Tozer, D. J.; Handy, N. C. *J. Chem. Phys.* **1998**, *109*, 10180.
(19) Tozer, D. J.; Handy, N. C. *J. Chem. Phys.* **1998**, *108*, 2545. Tozer, D. J.; Handy, N. C. *J. Phys. Chem. A* **1998**, *102*, 3162.
(20) Williams, H. L.; Szalewicz, K.; Jeziorski, B.; Moszynski, R.; Rybak, S. *J. Chem. Phys*. **1993**, *98*, 1279.
(21) Jankowski, P.; Szalewicz, K. *J. Chem. Phys.* **1998**, *108*, 3554.
(22) Mas, E.; Szalewicz, K.; Bukowski, R.; Jeziorski, B. *J. Chem. Phys.* **1997**, *107*, 4207.
(23) Williams, H. L.; Mas, E. M.; Szalewicz, K.; Jeziorski, B. *J. Chem. Phys.* **1995**, *103*, 7374.
(24) Williams, H. L. Ph.D. Dissertation, University of Delaware, Newark, DE, 1995.
(25) Williams, H. L.; Korona, T.; Bukowski, R.; Jeziorski, B.; Szalewicz, K. *Chem. Phys. Lett.* **1996**, *262*, 431.
(26) Korona, T.; Williams, H. L.; Bukowski, R.; Jeziorski, B.; Szalewicz, K. *J. Chem. Phys.* **1997**, *106*, 5109.
(27) Jeziorski, B.; Chalasinski, G.; Szalewicz, K. *Int. J. Quantum Chem.* **1978**, *14*, 271.
(28) Jeziorska, M.; Jeziorski, B.; Cizek, J. *Int. J. Quantum Chem.* **1987**, *32*, 149.
(29) Boys, S. F.; Bernardi, R. *Mol. Phys.* **1970**, *19*, 553.
(30) Jeziorski, B.; Szalewicz, K. "Intermolecular Interactions by Perturbation Theory", In *Encyclopedia of Computational Chemistry*; Schleyer, P. v. R, Allinger, N. L., Clark, T., Gasteiger, J., Kollman, P. A., Schaefer, H. F., III, Schreiner, P. R., Eds.; Wiley: Chichester, U.K., 1998; Vol. 2, p 1376.
(31) Lacks, D. J.; Gordon, R. G. *Phys. Rev. A* **1993**, *47*, 4681.
(32) Gordon, R. G.; Kim, Y. S. *J. Chem. Phys.* **1972**, *56*, 3122.
(33) Spackman, M. A. *J. Chem. Phys.* **1986**, *85*, 6579.
(34) Kolos, W.; Radzio, E. *Int. J. Quantum Chem.* **1978**, *13*, 627.
(35) Radzio-Andzelm, E. *Int. J. Quantum Chem.* **1981**, *20*, 601.
(36) Radzio-Andzelm, E. *Chem. Phys. Lett.* **1981**, *84*, 64.
(37) Jeziorski, B.; Bulski, M.; Piela, L. *Int. J. Quantum Chem.* **1976**, *10*, 281.
(38) Rapcewicz, K.; Ashcroft, N. W. *Phys. Rev. B* **1991**, *44*, 4032.
(39) Andersson, Y.; Langreth, D. C.; Lundqvist, B. I. *Phys. Rev. Lett.* **1995**, *76*, 102.
(40) Lundqvist, B. I.; Andersson, Y.; Shao, H.; Chan, S.; Langreth, D. C. *Int. J. Quantum Chem.* **1995**, *56*, 247.
(41) Dobson, J. F.; Dinte, B. P. *Phys. Rev. Lett.* **1996**, *76*, 1780.
(42) Casimir, H. B. G.; Polder, D. *Phys. Rev.* **1948**, *73*, 360.
(43) Kohn, W.; Meir, Y.; Makarov, D. E. *Phys. Rev. Lett*. **1998**, *80*, 4153.
(44) Stefanovich, E. V.; Truong, T. N. *J. Chem. Phys.* **1996**, *104*, 2946.
(45) Wesolowski, T. A.; Weber, J. *Chem. Phys. Lett.* **1996**, *248*, 71.
(46) Cioslowski, J.; Lopez-Boada, R. *J. Chem. Phys*. **1998**, *109*, 4156.
(47) Szabo, A.; Ostlund, N. S. *Modern Quantum Chemistry: Introduction to Advanced Electronic Structure Theory*; Macmillan Publishing Co., New York, 1982.
(48) Janak, J. F. *Phys. Rev. B* **1978**, *18*, 7165.
(49) Perdew, J. P.; Levy, M. *Phys. Rev. Lett.* **1983**, *51*, 1884.
(50) Gaussian 94, Revision D.2, Frisch, M. J.; Trucks, G. W.; Schlegel, H. B.; Gill, P. M. W.; Johnson, B. G.; Robb, M. A.; Cheeseman, J. R.; Keith, T.; Petersson, G. A.; Montgomery, J. A.; Raghavachari, K.; Al-Laham, M. A.; Zakrzewski, V. G.; Ortiz, J. V.; Foresman, J. B.; Cioslowski, J.; Stefanov, V.; Nanayakkara, A.; Challacombe, M.; Peng, C. Y.; Ayala, P. Y.; Chen, W.; Wong, M. W.; Andres, J. L.; Replogle, E. S.; Gomperts, R.; Martin, R. L.; Fox, D. J.; Binkley, J. S.; Defrees, D. J.; Baker, J.; Stewart, J. P.; Head-Gordon, M.; Gonzalez, C.; Pople, J. A.; Gaussian, Inc., Pittsburgh, PA, 1995.
(51) Jeziorski, B.; Moszynski, R.; Ratkiewicz, A.; Rybak, S.; Szalewicz, K.; Williams, H. L. In *Methods and Techniques in Computational Chemistry, METECC94, B, Medium-Size Systems*, Clementi, E., Ed.; STEF: Cagliari, 1993; p 79. The SAPT suite of codes is also available directly from the authors. For more information contact Krzysztof Szalewicz, Department of Physics and Astronomy, University of Delaware, Newark, DE 19716 or by email at szalewic@udel.edu.
(52) Becke, A. D. *J. Chem. Phys.* **1993**, *98*, 5648.
(53) Slater, J. C. *Quantum Theory of Molecules and Solids. Vol. 4: The Self-Consistent Field for Molecules and Solides*, McGraw-Hill: New York, 1974.
(54) Becke, A. D. *Phys. Rev. A* **1988** *38*, 3098.
(55) Vosko, S. H.; Wilk, L.; Nusair, M. *Can. J. Phys.* **1980**, *58*, 1200.
(56) Lee, C.; Yang, W.; Parr, R. G. *Phys. Rev. B* **1988**, *37*, 785.
(57) Miehlich, B.; Savin, A.; Stoll, H.; Preuss, H. *Chem. Phys. Lett.* **1989**, *157*, 200.
(58) Perdew, J. P.; Wang, Y. *Phys. Rev. B* **1992**, *45*, 13244.
(59) Williams, H. L.; Chabalowski, C. F. *J. Phys. Chem. A* **1998**, *102*, 6981.
(60) Bukowski, R.; Szalewicz, K.; Chabalowski, C. F. *J. Phys. Chem. A* **1999**, *103*, 7322.
(61) Dunning, T. H., Jr. *J. Chem. Phys.* **1989**, *90*, 1007.
(62) Kendall, R. A.; Dunning, T. H., Jr.; Harrison, R. J. *J. Chem. Phys.* **1992**, *96*, 6796.
(63) Woon, D. E.; Dunning, T. H., Jr. *J. Chem. Phys.* **1993**, *98*, 1358.
(64) Grabo, T.; Kreibich, T.; Kurth, S.; Gross, E. K. U. *Strong Coulombic correlations in electronic structure calculations: beyond the Local Density Approximation*, Anisimov, V. I., Ed.; Gordon and Breach: Amsterdam, May, 2000.
(65) Slater, J. C. *Phys. Rev.* **1951**, *81*, 385.
(66) Williams, A. R.; deGroot, R. A.; Sommers, C. B. *J. Chem. Phys.* **1975**, *63*, 628.
(67) Levy, M. *Phys. Rev. A* **1995**, *52*, R4313.